You might find this additional information useful...

Supplemental material for this article can be found at:
http://ajpcell.physiology.org/cgi/content/full/00303.2007/DC1

This article cites 38 articles, 20 of which you can access free at:
http://ajpcell.physiology.org/cgi/content/full/294/1/C333#BIBL

This article has been cited by 1 other HighWire hosted article:

Loss of the apical V-ATPase a-subunit VHA-6 prevents acidification of the intestinal lumen during a rhythmic behavior in C. elegans
E. Allman, D. Johnson and K. Nehrke
Am J Physiol Cell Physiol, November 1, 2009; 297 (5): C1071-C1081.
[Abstract] [Full Text] [PDF]

Updated information and services including high-resolution figures, can be found at:
http://ajpcell.physiology.org/cgi/content/full/294/1/C333

Additional material and information about *AJP - Cell Physiology* can be found at:
http://www.the-aps.org/publications/ajpcell

This information is current as of July 8, 2010 .

Intestinal Ca^{2+} wave dynamics in freely moving *C. elegans* coordinate execution of a rhythmic motor program

K. Nehrke,[1] Jerod Denton,[2] and William Mowrey[3]

[2]*Departments of Anesthesiology and Pharmacology, Digestive Disease Research Center, Vanderbilt University Medical Center, Nashville, Tennessee; and* [3]*Interdepartmental Graduate Program in Neuroscience, Center for Aging and Developmental Biology and* [1]*Nephrology Division, Department of Medicine, University of Rochester Medical Center, Rochester, New York*

Nehrke K, Denton J, Mowrey W. Intestinal Ca^{2+} wave dynamics in freely moving *C. elegans* coordinate execution of a rhythmic motor program. *Am J Physiol Cell Physiol* 294: C333–C344, 2008. First published October 17, 2007; doi:10.1152/ajpcell.00303.2007.—Defecation in the nematode worm *Caenorhabditis elegans* is a highly rhythmic behavior that is regulated by a Ca^{2+} wave generated in the 20 epithelial cells of the intestine, in part through activation of the inositol 1,4,5-trisphosphate receptor. Execution of the defecation motor program (DMP) can be modified by external cues such as nutrient availability or mechanical stimulation. To address the likelihood that environmental regulation of the DMP requires integrating distinct cellular and organismal processes, we have developed a method for studying coordinate Ca^{2+} oscillations and defecation behavior in intact, freely behaving animals. We tested this technique by examining how mutations in genes known to alter Ca^{2+} handling [including *egl-8*/phospholipase C (PLC)-β, *kqt-3*/KCNQ1, *sca-1*/sarco (endo)plasmic reticulum Ca^{2+} ATPase, and *unc-43*/Ca^{2+}-CaMKII] contribute to shaping the Ca^{2+} wave and asked how Ca^{2+} wave dynamics in the mutant backgrounds altered execution of the DMP. Notably, we find that Ca^{2+} waves in the absence of PLCβ initiate ectopically, often traveling in reverse, and fail to trigger a complete DMP. These results suggest that the normal supremacy of the posterior intestinal cells is not obligatory for Ca^{2+} wave occurrence but instead helps to coordinate the DMP. Furthermore, we present evidence suggesting that an underlying pacemaker appears to oscillate at a faster frequency than the defecation cycle and that arrhythmia may result from uncoupling the pacemaker from the DMP rather than from disrupting the pacemaker itself. We also show that chronic elevations in Ca^{2+} have limited influence on the defecation period but instead alter the interval between successive steps of the DMP. Finally, our results demonstrate that it is possible to assess Ca^{2+} dynamics and muscular contractions in a completely unrestrained model organism.

calcium; oscillation; *Caenorhabditis elegans*; biosensor

CA^{2+} IS A VERSATILE INTRACELLULAR second messenger, and Ca^{2+} signals are regulated at the molecular level by a vast array of mechanisms (for review, see Ref. 1). The spatial and temporal patterns of Ca^{2+} signals as well as the molecular machinery used to interpret those signals help to determine the functional output of individual Ca^{2+} signaling pathways. One particularly important way in which biological systems use Ca^{2+} to transmit information is oscillatory Ca^{2+} signaling. Rhythmic Ca^{2+} oscillations regulate a variety of different biological processes, such as oocyte activation, growth cone migration, muscle development, and pathogenic responses (10, 11, 26, 34). Fur-

thermore, oscillatory Ca^{2+} flux may be involved in timing cyclic behavior, such as ultradian rhythms, which occur with less than a 24-h period (examples include gut peristalsis, breathing, and the beating of a heart).

The nematode *Caenorhabditis elegans* is a genetic model organism that exhibits a rhythmic defecation behavior that is timed by Ca^{2+} signaling (for review, see Ref. 2). The wild-type hermaphrodite executes a defecation motor program (DMP) at ~45-s intervals in the presence of food (18, 32). The DMP is highly stereotyped, consisting of three consecutive sets of muscular contractions (32). Initiation of the cycle occurs as the intestinal contents are pressurized by a simultaneous contraction of both dorsal and ventral posterior body wall muscles (pBoc). This is followed several seconds later by contraction of the anterior body wall muscles (aBoc), which drives the pharynx in the intestine and moves the contents of the lumen backward. Finally, a group of muscles around the anus is responsible for expulsion (Exp).

The timing and rhythm of the defecation cycle is remarkably consistent, with all of the hallmarks of a molecular clock. A genetic screen for defecation timing mutants identified the gene *itr-1*, which encodes the single worm inositol 1,4,5-trisphosphate receptor (IP_3R), an intracellular Ca^{2+} release channel (32). The phenotypic effects of *itr-1* on defecation were shown to be conveyed via its activity in the 20 epithelia cells that comprise the worm intestine (32), and mutations in the *itr-1* gene or overexpression of the IP_3R in the intestine affected cycle timing (6), whereas expression of an IP_3 "sponge" disrupted defecation (35). Finally, optical recordings using the Ca^{2+}-sensitive dye fura 2 revealed that activation of the DMP correlates with an elevation in Ca^{2+} in posterior intestinal cells (6), suggesting that Ca^{2+} signals in the intestine comprise part of the defecation clock.

Recently, several laboratories have employed a combination of genetics and physiology to lend further insight to the molecular mechanisms that regulate rhythmic Ca^{2+} oscillations in the intestinal epithelia. The laboratory of Dr. K. Strange has developed a system for studying Ca^{2+} signals in partially isolated intestines. They demonstrated that a Ca^{2+} wave initiates rhythmically at the posterior end of the intestine and propagates toward the anterior end with a period similar to that of the defecation cycle (7). Furthermore, they showed that two of the six individual worm phospholipase C (PLC) genes, whose products generate inositol 1,4,5-trisphosphate (IP_3) and

diacylglycerol (DAG) from the hydrolysis of phosphatidylinositol 4,5-bisphosphate (PIP$_2$), help to maintain the defecation rhythm through genetically separate pathways (7). Along similar lines, the laboratory of Dr. K. Iwasaki developed a system for imaging Ca^{2+} using a yellow cameleon expressed in the intestine of intact worms that have been immobilized on agarose pads and showed, in this experimental model, that posterior-to-anterior Ca^{2+} waves in the intestine coincided with activation of the DMP (31). The molecular mechanisms that mediate the propagation of this Ca^{2+} wave are not well understood, although the work of the Teramoto and Iwasaki (31) demonstrated that wave propagation is required to trigger the aBoc and Exp steps of the DMP.

Significantly, the dynamics of Ca^{2+} wave propagation have not previously been investigated under physiological conditions, and it is currently unknown whether observations from existing models reflect normal physiology. This is an important concern, since the execution of the DMP is known to be regulated in response to mechanical stimuli and food-related sensory cues (3, 18, 29, 32). Here, we describe a system that we have developed for following Ca^{2+} waves in intact, freely behaving worms using a transgenic YC6.1 biosensor. Under these conditions, worms exhibited a normal, rhythmic activation of the DMP that coincided with Ca^{2+} wave propagation through the intestine. However, Ca^{2+} wave dynamics were distinct from those observed in restrained or reduced preparations: the wave initiated simultaneously from both the anterior and posterior intestinal cells and propagated inward. We found that genetic perturbations associated with arrhythmia in the defecation cycle disrupt the propagation of this wave in specific ways. Loss of PLC-B altered both the timing and the site of Ca^{2+} wave initiation, whereas disrupting KCNQ K$^+$ channel function severely impaired the ability of the wave to propagate. Furthermore, the disruption of CaM-CaMKII signaling increased the frequency of wave propagation, resulting in the reiteration of the DMP at less than a normal cycle length. Surprisingly, we also found that increasing the duration of cellular Ca^{2+} oscillations through reduction in sarco(endo)plasmic reticulum Ca^{2+} ATPase (SERCA) function did not extend the cycle period appreciably but instead disrupted the coordination between sequential muscular contractions. Based on our results, we propose a model where Ca^{2+} waves are shaped spatially by their specific cellular foci of initiation and temporally by an underlying, higher-frequency oscillator. Taken together, these findings demonstrate the power of our system to elucidate the molecular mechanisms controlling ultradian rhythms and the propagation of Ca^{2+} waves in an awake, behaving animal.

METHODS

Nematode culture and genetics. Worm strains were propagated at 15°C or 20°C on normal growth media (NGM) agar plates containing 5 μg/ml cholesterol and seeded with OP50 bacteria. Methods for culturing, handling, and genetics were generally as described by Brenner, (3a). The strains used in this work are as follows: KWN1, *pha-1(e2123ts)III*; *rnyEx001* [*pKT2-nhx2* (*nhx-2p::*YC6.1), *pCL1* (*pha-1*)], and the following strains, which contain the mutations indicated, in addition to *pha-1(e2123ts)III; rnyEx001*; KWN2, *unc-31(n422)IV*; KWN3, *egl-8(n488)V*; KWN4, *kqt-2(tm642)X*; KWN5, *kqt-3(tm542)II*; KWN6 *unc-43(sa200)IV*; KWN7, *unc-54(e190)I*; KWN14, *itr-1(sa73)IV*. Also used were KWN15, *rde-1(ne219)V; rnyEx002* [*pXXY2004.1(nhx-2p::RDE-1)*],

pKT2-nhx2 (*nhx-2p::*YC6.1)*, pRF4* [*rol-6(su1006)*], and KWN16, *pha-1(e2123ts)III*; *rnyEx003* [*nhx-2p::YC2.12, pCL1(pha-1)*].

Strains were made available by the *C. elegans* Genetics Center. The deletion mutants were obtained from S. Mitani at the *C. elegans* National BioResource Project in Japan. Each deletion strain was crossed to N2 wild-type worms three times before use. The deletion break points have been mapped, which allowed us to formulate a PCR-based genotyping assay that includes three primers for each strain, two of which flank the deletion and one of which anneals within the deleted sequences. For *kqt-2* genotyping, the primer sequences are as follows: forward 1 (F1): ACTTTTCCCTTAGTTTCT-TCGCAAG; forward 2 (F2): CCGTTGTCTTGAATTCCTTGAGC; and reverse 1: TGGGACTCTGCTGTTTTACGC. The wild-type PCR product(s) are 309 and 1180 nucleotides long, whereas the tm642 allele produces a 379 nucleotide product. For *kqt-3* genotyping, the primer sequences are as follows: F1: TTGTCTAGAACGC-CCGACTG; R1: TTTGGGAAGCAGCCGACATC; and reverse 2: TCCTAAAACCGCGCCTTGTAG. The wild-type PCR product(s) are 457 and 1458 nucleotides long, whereas the tm542 allele produces a 261 nucleotide product. In most cases, the shorter wild-type genomic PCR product was preferentially amplified over the longer product, as would be expected.

RNA interference. Freshly transformed colonies of the bacterial strain HT115 were grown to midlog phase at 37°C and induced for 1 h with 1 mM IPTG. After fivefold concentration, 80 μl of bacteria were added to the surface of 35- or 60-mm NGM agar or agarose plates supplemented with cholesterol and 0.1 mM IPTG. Later (2 days), L3 larvae were placed on the RNAi plates for 36 h before being moved to a fresh plate, where they were allowed to lay eggs. These progeny were then used for further experiments.

Vectors and creation of transgenic strains. RNAi vectors were created by PCR cloning of from 600 to 1000 nucleotides of the coding region from the target gene in the Fire lab double-strand RNA feeding vector pPD129.36 (Courtesy of A. Fire, Stanford University). The vector pKT2 is a derivative of pFH6.II (14) containing the YC6.1 open reading frame (ORF) in place of green fluorescent protein (GFP). The vector pXXY2004.1, containing the RDE-1 ORF, was a kind gift from K. Strange (Vanderbilt University). The *nhx-2* promoter (24) was used in these vector backbones to drive the expression of RDE-1 and YC6.1 specifically in the intestine. Anti-GFP positive and anti-*pos-1*negative controls were used to verify cell-specific RNAi in this strain (data not shown). Furthermore, *vav-1(RNAi)* worms were shown to have a modest arrhythmia [coefficient of variation (COV) of 43.9 ± 31.0%], as demonstrated previously (25), whereas *itr-1(RNAi)* worms were viable, suggesting the absence of RNAi in the gonadal sheath cell, but had defecation frequencies of >5 min because of a lack of Ca^{2+} oscillations (Table 1).

To create transgenic strains containing extrachromosomal arrays, constructs were mixed with either pCL1, which rescues the *pha-1(e2131ts)III* allele (13), or pRF4, which encodes a dominant *rol-6* mutation, at 75 μg/ml each in high-potassium injection buffer and then coinjected in the gonad of either *pha-1(e2131ts)III* or *rde-1(ne219)V* mutants, as described previously (21). After 4 days at 22°C, F$_1$ progeny were examined for germline transmission. Ultraviolet irradiation of a mosaic line, followed by extensive outcrossing, resulted in the generation of a highly stable, but not integrated, extrachromosomal array for the YC6.1 reporter.

Ca^{2+} imaging. Transgenic nematode larva (generally L3-L4 larva) expressing YC6.1 from the *nhx-2* promoter in the intestine were imaged on 60-mm NGM-agarose plates (±IPTG for RNAi) seeded with ⅕ the amount of bacteria normally used, since the bacteria, like agar, can increase the background fluorescence. Optical recordings were performed on a Nikon 2000U inverted microscope coupled to a monochromatic light source (Polychrome IV; Till Photonics), CCD camera detection system (Cooke, Germany), and optical beamsplitter (Optical Insights, Tucson, AZ). Nikon Plan Apo ×10 [0.5 numeric

Table 1. *Cycle period, rhythmicity, and coordination of defecation motor program*

Allele	Array	RNAi	pBoc Period, s	pBoc CV, %	pBoc to aBoc Interval, s	pBoc to aBoc CV, %
Control *N2*	NA	NA	49.5±7.4	6.4±3.4	4.5±0.5	10.8±1.6
unc-31(n422)	NA	NA	51.9±5.4	5.0±1.8	5.3±0.9	9.7±6.2
unc-31(n422), pha-1(e2123ts)	NA	NA	53.7±4.4	5.2±0.8	5.3±0.2	12.1±3.0
pha-1(e2123ts)	rnyEx001	NA	60.2±2.3	5.3±2.6	6.2±0.4	8.4±2.0
*unc-31(n422), pha-1(e2123ts)**	rnyEx001	NA	57.0±3.2*	8.6±2.6*	5.4±0.5*	3.2±1.3*
egl-8(n488), pha-1(e2123ts)	rnyEx001	NA	71.6±12.1	33.1±10.7	ND	ND
kqt-2(tm642)	NA	NA	83.0±4.0	14.0±4.0	7.8±0.8	10.6±1.4
kqt-3(tm542)	NA	NA	156.0±10.0	24.0±6.0	8.0±0.8	9.7±1.7
rde-1(ne219)	NA	NA	64.8±11.5	6.8±3.7	5.1±0.6	11.7±2.0
rde-1(ne219)	rnyEx002	NA	65.3±9.4	10.4±4.2	4.2±0.4	4.6±10.2
rde-1(ne219)	rnyEx002	*vav-1*	122.6±26.5	43.9±31.0	4.0±0.8	12.1±8.4
rde-1(ne219)	rnyEx002	*sca-1*	73.2±11.8	7.7±2.8	19.1±15.4	9.6±4.9
rde-1(ne219)	rnyEx002	*egl-8*	80.7±18.7	36.2±9.9	ND	ND
rde-1(ne219)	rnyEx002	*itr-1*	>300	ND	ND	ND

Values are means ± SD calculated from 5 worms followed under a stereomicroscope for five defecation cycles. pBoc, posterior body wall muscle; aBoc, anterior body wall muscle; CV, coefficient of variation. Extrachromosomal arrays were maintained by coinjection of the *rol-6* dominant marker or via *pha-1* rescue as follows: rnyEx001 is [pKT2-nhx2 (*nhx-2*p::YC6.1), pCL1(*pha-1*)]; Ex002 is [pXXY2004.1 (*nhx-2*p::RDE-1), pKT2-nhx2 (*nhx-2*p::YC6.1), pRF4 (*rol-6 (su1006)*]. *Data obtained directly from fluorescent images analyzed post hoc. NA, not available; ND, not determined.

aperture (NA)] or ×20 (0.85 NA) air objectives were used for routine imaging.

For YC6.1 acquisitions, we used a 40- to-100-ms exposure time and 4- to 20-Hz frame rates. The fluorescence intensity of YC6.1 was generally homogenous throughout the intestinal cells, and the reporter generated a signal-to-background ratio of at least five at each emission wavelength. After excitation at 435 nm, the emissions were acquired and saved simultaneously at both 480 and 535 nm using TILLvisION software (TILL Photonics). Background emission images were generated using the same acquisition settings and subtracted from each experimental image on a pixel-by-pixel basis. FRET measurements were calculated using the TILLvisION FRET module, which generates an emission ratio (R) image overlay. With the above acquisition parameters, thresholding the overlay to a minimum pixel density of approximately one-half the background value eliminated nonspecific or weak signals so that only the intestine was visible. Intestinal cells were outlined using a single channel emission image as a guide and then updated in successive images to account for movement. Cellular Ca^{2+} dynamics were determined by R/R_0, using a series of four to eight frames before defection to normalize the emission ratios. pBoc was denoted post hoc from the image series as a pBoc contraction of the intestine and aBoc as a depression of the pharynx in the lumen of the intestine, which displaces the anteriormost segment of int-1. Similarly, Exp was marked by a short (0.25–0.50 s) contraction of the enteric muscles. The ratio change in the YC6.1 reporter was ~1.6-fold from minimum to maximum Ca^{2+} (data not shown).

Analysis of pBoc and pharynx pumping. pBoc was monitored at room temperature in either L4 larval (Table 1) or 2-day-old adult worms (see Fig. 3) swimming on a lawn of OP-50 bacteria grown on agar plates. Worms were imaged using a Carl Zeiss MicroImaging Stemi SV11 M²BIO stereo dissecting microscope (Kramer Scientific) equipped with a DAGE-MTI DC2000 CCD camera or Nikon SMZ 800 stereo dissecting microscope. pBoc rhythmicity in individual worms was assessed by calculating the coefficient of variance (CV), which is the SD of the pBoc period expressed as a percent of the mean, from 10 successive contractions.

Pharynx pumping in individual worms was imaged using the same microscope apparatus described above and recorded using a Pioneer Elite DVR-7000 recorder. Pharynx pumping was replayed at slow speed, and pharynx pumps over 60 s were manually counted. Pharynx pumping CV was determined as described above.

RESULTS

Two converging intestinal Ca^{2+} waves occur during activation of the DMP. To study intestinal Ca^{2+} dynamics in live worms, the yellow cameleon YC6.1 (33) was expressed under the control of the intestinal *nhx-2* promoter (24). The resulting strain had a defecation period that was slightly longer than normal, which may be because of Ca^{2+} buffering by the YC6.1 reporter (Table 1). However, because execution of the DMP was normal in both its rhythm and execution, we concluded that this strain was a valid model to study intestinal Ca^{2+} oscillations during defecation.

Previous studies using isolated intestines or immobilized animals have shown that a Ca^{2+} wave propagates through the intestine from the posterior to anterior end (7, 31). However, we observed inconsistent muscular contractions and poorly propagating waves when the worms were immobilized (Supplemental Fig. S1; Supplemental data for this report may be found on the *American Journal of Physiology: Cell Physiology* web site.). We therefore measured Ca^{2+} using low-power air objectives to follow live nematodes on an agarose plate under normal physiological conditions, which we term "free range" imaging. Like the system implemented by Faumont et al. (8, 9) to characterize behavioral responses to Ca^{2+} flux in chemosensory neurons of partially restrained worms, this protocol allowed us to observe the integration of Ca^{2+} flux, muscular contractions, and neural modulation of the DMP in intact, living animals.

Imaging was facilitated by crossing an "uncoordinated" *unc-31(n422ts)* allele in the Ca^{2+} reporter strain. *Unc-31* encodes a Ca^{2+} activator of protein secretion that functions in the $G_{\alpha}s$ pathway in cholinergic motor neurons to regulate locomotion (4). The *n422ts* allele is temperature sensitive, produces a relatively mild deficit at 20°C, the temperature of our assays, and has normal defecation cycle timing and execution (Table 1). In addition, intestinal calcium dynamics in the *unc-31(n422ts)* background were indistinguishable from wild-type controls (data not shown).

Execution of the DMP and intestinal Ca^{2+} oscillations occurred simultaneously (Fig. 1*A* and Table 1), as predicted
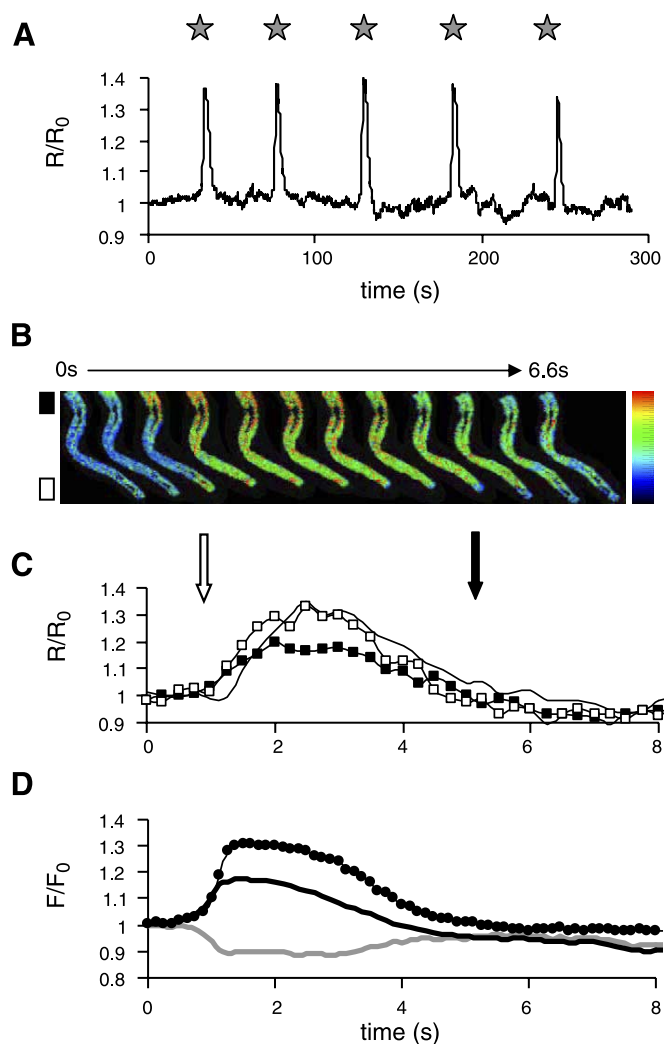
Fig. 1. Intestinal Ca^{2+} dynamics during defecation in "free-range" worms. *A*: intracellular Ca^{2+} oscillations in unstrained nematodes over 5 min. The 535/480 nm emission ratio of YC6.1 following 435 nm excitation was averaged throughout the entire intestine and normalized to the starting ratio. The single channel emission images obtained at 535 nm were used to denote defecation motor program (DMP) execution post hoc (stars). *B*: this time lapse of pseudocolored YC6.1 535/480 nm emission ratio maps was obtained by extracting every third image from a 5-Hz acquisition series during defecation. The worm is oriented with the head facing up. *C*: analysis of Ca^{2+} flux in the anterior (■) and posterior (□) intestine, with the regions-of-interest corresponding to black and white boxes diagramed in the image series ($n = 3$). Values taken from a region near the middle of the intestine are plotted as a solid line. The arrows denote the start of posterior body wall (pBoc; white) and anterior body wall (aBoc; black) muscular contractions. *D*: ratio of emissions (●) from YC6.1 reflects an inversely proportional relationship between single channel emission intensities (480 nm in gray, 535 nm in black), which are characteristic of FRET, and a conformation change that occurs in the biosensor as Ca^{2+} rises.

from the existing model (6, 7, 25, 31). Muscular contractions could be readily observed post hoc, and, as shown in Table 1, the average defecation period and rhythm calculated from these calcium oscillations were indistinguishable from those determined visually under a dissecting microscope.

The ratio map of yellow fluorescent protein (YFP)/cyan fluorescent protein (CFP) fluorescent emissions from YC6.1 in Fig. 1*B* is representative of the Ca^{2+} wave routinely observed during defecation ($n > 50$ worms). Although it has been suggested that a single Ca^{2+} wave progresses posterior-to-

anterior through the intestine (31), we instead observed two waves that initiated at both the anterior and posterior ends of the intestine and converged (Fig. 1*B* and Supplemental Movie S1). To quantify the temporal and spatial characteristics of these waves, regions of interest were drawn around groups of intestinal cells using a single channel emission image as a guide, and R/R₀ values for the YFP/CFP emission ratio were determined (Fig. 1, *B* and *C*). These regions of interest were updated manually as the worm moved or as contractions occurred until defecation was complete. The muscular contractions were denoted post hoc by examining single channel emission recordings as stated.

Ca^{2+} waves initiated from both ends of the intestine nearly simultaneously and propagated through the entire organ in <1 s (Fig. 1, *B* and *C*). Ca^{2+} remained elevated for ~4 s, with the anterior and posterior cells returning to baseline before cells located more centrally. pBoc coincided with the elevated Ca^{2+} in the posterior cells, whereas aBoc appeared to occur as Ca^{2+} returned to baseline in the anterior cells, suggesting that contractions of the aBoc are not simply triggered by high Ca^{2+}. Evidence of FRET was reflected by the inverse relationship between the single channel emission intensities during a rise in Ca^{2+} (Fig. 1*D*) in both the anterior and posterior cells, suggesting that the "backward" wave does not reflect some unaccounted for environmental sensitivity of YC6.1. Moreover, we generated a strain expressing the cameleon YC2.12 such as was used previously (31) and, employing our free range technique, found the same pattern of dual initiation and convergent propagation as shown in Fig. 1 (Supplemental Fig. S2); in fact, we observed convergent Ca^{2+} waves in every mutant background used in this manuscript (see below). At present, we cannot reconcile these observed differences, other than to comment on distinct imaging techniques. However, we agree fully with the previous observation that the posterior-to-anterior wave is necessary for coupling and execution of the complete DMP, as shown below.

PLCβ regulates the site of Ca^{2+} wave initiation. Recent reports have identified several gene products that function upstream of the IP₃R in the intestine to regulate the production of IP₃, and reducing their function can lead to cycle length defects as well as arrhythmia (7, 16, 25). These include PLCγ, which generates IP₃ and DAG from the hydrolysis of membrane lipid PIP₂, and loss of the PLCγ coding gene *plc-3* can be suppressed by a gain-of-function mutation in *itr-1* that reduces reliance upon upstream signaling pathways (8). However, the nematode PLCβ ortholog EGL-8 apparently works through a mechanism distinct from PLC-3, since an *itr-1* gain-of-function cannot suppress arrhythmia in the *egl-8(n488)* mutant.

Intestinal Ca^{2+} oscillations were arrhythmic and occurred with reduced amplitude in the *egl-8(n488)* mutant (Fig. 2*A*), similar to the oscillations observed previously in isolated intestines (7), and consistent with arrhythmic defecation (Table 1). However, instead of coordinated initiation at the anterior and posterior ends of the intestine, the mutant worms exhibited random increases in Ca^{2+} that propagated from cell to cell in the form of a wave, but often in the wrong direction, as shown by the representative image series in Fig. 2*C*. Out of approximately 20 mutant worms imaged, all displayed seemingly random oscillations, with approximately an equal probability of initiating at the anterior end, the posterior end, or in the

A

B

C

pBOC
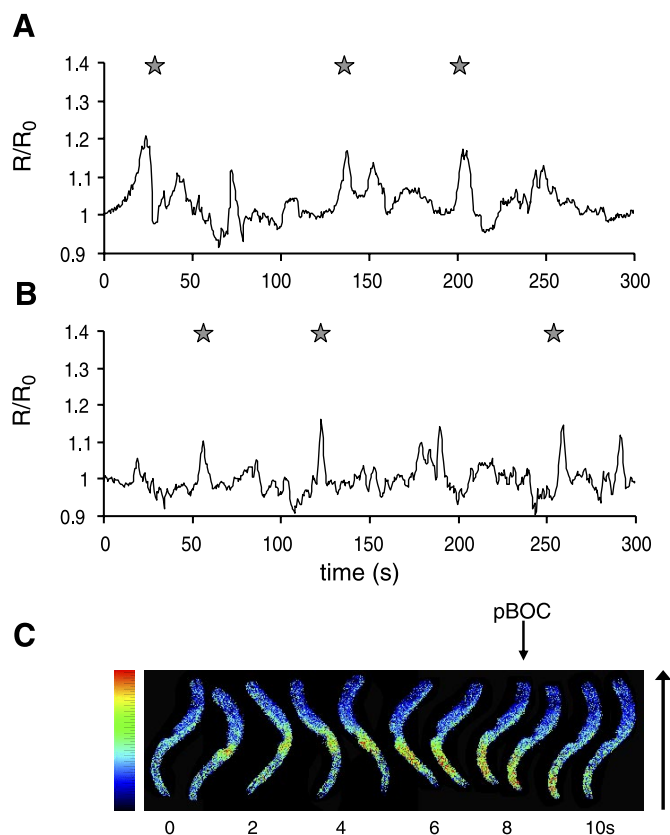
Fig. 2. Phospholipase C (PLC) β limits the site of Ca^{2+} wave initiation. *A*: intracellular Ca^{2+} oscillations were averaged throughout the entire intestine and normalized to the starting ratio for a representative *egl-8(n488)* mutant. *B*: Ca^{2+} oscillations were measured following intestinal cell restricted RNAi targeting of the *egl-8* gene product. The single channel emission images obtained at 535 nm were used to denote DMP execution post hoc (stars). *C*: cytoplasmic Ca^{2+} wave propagation in the intestine of an *egl-8(n488)* mutant. This 1-Hz series of YC6.1 emission ratio maps shows a Ca^{2+} wave initiating in the middle of the intestine, near int5, and propagating rearward, in the opposite direction as normally observed. The speed of the wave is abnormally slow, as well (compare with Fig. 1*B*). The worm is oriented with the head facing up, as shown by the black arrow.

middle of the intestine (data not shown). We hypothesize that previous observations of diminished muscular contractions in *egl-8* mutants (17) may have to do with reverse orientation waves such as these being able to elicit a pBoc contraction, albeit weakly. However, we never observed aBoc or Exp following a reverse wave. These observations strongly suggest that both the orientation and propagation of the Ca^{2+} wave(s) are required for contraction coupling. We further postulate that all intestinal cells are capable of initiating Ca^{2+} waves and that PLCβ reinforces the supremacy of the posterior cells as the defecation pacemaker.

EGL-8 has also been shown to participate in signaling at neuromuscular junctions (17). To directly test if EGL-8 regulates Ca^{2+} oscillation/wave initiation in intestinal cells through cell-autonomous mechanisms, we used cell type-specific RNA interference of intestinal EGL-8 as reported previously (7). In short, the *rde-1(ne219)* mutant is resistant to RNAi: we rescued RDE-1 activity exclusively in the intestine by driving its expression via the *nhx-2* promoter and included the YC6.12 reporter in the transgenic array to be able to measure Ca^{2+}. Both the parent and transgenic *rde-1* strains had slightly

increased defecation periods compared with N2 worms, although the difference barely reached significance (P = 0.048). Control RNAi treatments that demonstrate the efficacy and specificity of the strain are given in Table 1 and in Fig. 6. We found that intestinal *egl-8(RNAi)* caused the same defecation phenotype as the *egl-8(n488)* mutation (Fig. 2*B* and Table 1). This suggests that EGL-8 limits intestinal cell Ca^{2+} wave initiation through cell intrinsic activity.

KCNQ M-type K⁺ channels are essential for Ca^{2+} wave propagation. In vertebrate systems, KCNQ M-type K⁺ channels play an important role in the regulation of ultradian rhythms, such as heart beat and electroencephalogram theta rhythm, in cardiomyocytes and neurons. These channels are also prominently expressed in several epithelial tissues, where their roles are less well understood. The nematode genome encodes three KCNQ K⁺ channel homologs termed KQT-1-3 (36). Notably, specific isoforms of KQT-2 and KQT-3 are known to be expressed in the worm intestine, where they may serve to regulate the dynamics of Ca^{2+} waves. It has been demonstrated previously that Ca^{2+} entry from outside the cell is required for Ca^{2+} oscillations in the worm intestine, although the mechanism of Ca^{2+} entry is not currently known (19, 37). In nonexcitable cells such as the worm enterocyte, KNCQ channels can potentially serve as important regulators of the rate of Ca^{2+} influx, since they can significantly influence the cell's membrane potential. We therefore decided to assess the role of the genes *kqt-2* and *kqt-3* in regulating oscillatory Ca^{2+} signaling and the execution of the DMP.

Both the *kqt-2(tm642)* and *kqt-3(tm542)* deletion alleles were associated with an increase in the defecation period (Fig. 3, *A*–*C* and Table 1). In contrast to the regular intervals at which Ca^{2+} oscillated in wild-type worms (Fig. 3*D*), both of these kqt loss-of-function mutations caused irregular oscillations, correlating with the increased COV for the defecation period (Fig. 3, *E* and *F*). However, the duration that Ca^{2+} remained elevated was longer than the wild type as well, and Ca^{2+} oscillations that did not provoke DMP execution were noted in both mutants (Figs. 3, *E* and *F*). These data are consistent with the idea that KQT channels have an important role in promoting Ca^{2+} oscillations in the intestine, possibly by controlling the electrical driving force on Ca^{2+} influx. The lengthened duration may reflect a slower influx of Ca^{2+}, whereas the nonproductive intermediate oscillations could result from failed wave propagation.

To test this hypothesis, we examined Ca^{2+} wave propagation. Significantly, the intermediate oscillations were found to be the result of Ca^{2+} waves initiating at the anterior end of the intestine and progressing slowly toward the posterior end, but without the corresponding posterior-to-anterior wave initiating (Fig. 4 and Supplemental Fig. S3), consistent with our observations of *egl-8* mutants in supporting the idea that the posterior-to-anterior wave is necessary to trigger DMP execution. Even more telling was the fact that, during normal defecation, posterior Ca^{2+} oscillations in the *kqt* mutants were invariably preceded, often at great length, by anterior oscillations (Fig. 3, *H* and *I*). This phenomenon could reflect inherent differences in the regulation of wave generation in the anterior and posterior cells of the intestine, such as a more prominent role for KQT channels in promoting generation of the posterior wave. Alternatively, there could be some dependency between the anterior and posterior oscillation events. Although we are
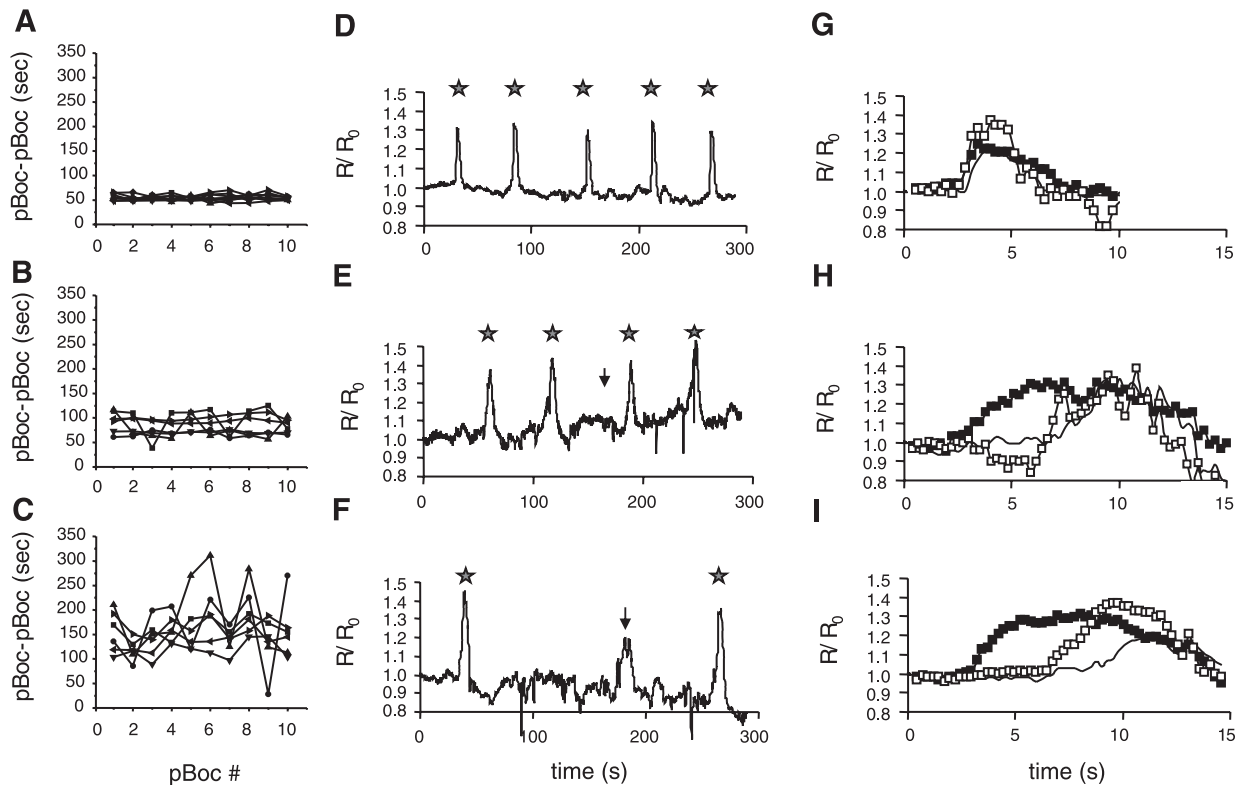
Fig. 3. KCNQ K⁺ channels and Ca²⁺ wave propagation. The DMP period was determined for N2 control (*A*), *kqt-2(tm642)* (*B*), and *kqt-3(tm542)* (*C*) mutants (2-day old adults) over 10 cycles (*n* = 6). Average intracellular Ca²⁺ oscillations are shown for representative N2 control (*D*), *kqt-2(tm642)* (*E*), and *kqt-3(tm542)* (*F*) mutants. Stars denote execution of the DMP, whereas the arrows in *E* and *F* represent times where elevations in Ca²⁺ occurred but were restricted to individual cells, did not propagate, and did not trigger the DMP. *G*, *H*, and *I* represent relative Ca²⁺ changes in anterior (■), posterior (□), and juxtauterine intestinal cells during defecation, as described above, for N2 control, *kqt-2(tm642)*, and *kqt-3(tm542)* mutants (*n* = 3), demonstrating that wave propagation occurs slowly in both mutants.

unable to ascribe a physiological function to the reverse wave, the fact that it uniformly precedes the posterior-to-anterior wave suggests that, if not necessary, it may at least be a harbinger of the DMP.

CaMKII suppresses intracycle Ca²⁺ oscillations: evidence for an underlying pacemaker activity? To further investigate the relationship between Ca²⁺ wave propagation and defecation rhythm, we examined wave propagation in the *unc-43(sa200)* mutant. UNC-43, the nematode ortholog of CaMKII, has an important role in controlling the rhythmic execution of the DMP, such that *unc-43* loss-of-function mutations cause a weak repetition or "shadow" of the DMP (18), whereas gain-of-function mutations inhibit Exp and lengthen the cycle period (28). Furthermore, unlike in wild-type worms, the DMP continues to be executed in the absence of food (18). These results led to the hypothesis by J. Thomas and colleagues that CaMKII may negatively regulate ITR-1-mediated Ca²⁺ spikes in the intestine.

The traces shown in Fig. 5, *A* and *B*, show intestinal Ca²⁺ oscillations over a single cycle from two representative *unc-43(sa200)* mutants. To portray the dynamics of the Ca²⁺ waves that occurred in these mutants, YC6.1 ratio emission images were extracted at the times indicated in each of the traces, as shown to the bottom. In one of the mutants (Fig. 5*A*), normal DMP execution (stars) was followed by reiteration of the DMP, or a shadow contraction, one-third of a cycle length later (thick arrow). The Ca²⁺ waves that occurred during this

shadow contraction were indistinguishable from those that coincided with normal DMP execution. However, there was extensive heterogeneity, both among worms and among successive cycles in the same worm, in the degree to which the shadow contractions occurred (18). The mutant in Fig. 5*B* had a very weak, almost unnoticeable, pBOC contraction, aBOC/Exp failed to occur, and the Ca²⁺ waves were reduced compared with the norm.

A second shadow DMP infrequently follows shadow cycles in *unc-43* mutants (28). Even in the absence of a second shadow, we observed a slight elevation in Ca²⁺ following most strong shadow cycles that occurred with a latency similar to that of the shadow itself (Fig. 5*A*). These oscillations together divided the defecation cycle into approximately equal thirds.

To ask whether CaMKII acts in the intestine to regulate Ca²⁺ oscillations, we first attempted intestine-restricted RNAi to limit loss-of-function to this tissue alone. However, we were unable to phenocopy the *unc-43(sa200)* mutation using feeding RNAi, which is unsurprising given that *unc-43* RNAi has failed to elicit any phenotype from the many global RNAi screens performed in worms and may thus be refractory to RNAi. To provide alternate suggestive evidence that UNC-43 may act in the intestine to regulate defecation, we adopted the following approach: we targeted intestinal *cmd-1*, the single worm calmodulin ortholog. The cycle period was extended by this treatment, and the oscillations were increased in duration, which is unsurprising given that *cmd-1* likely regulates multi-
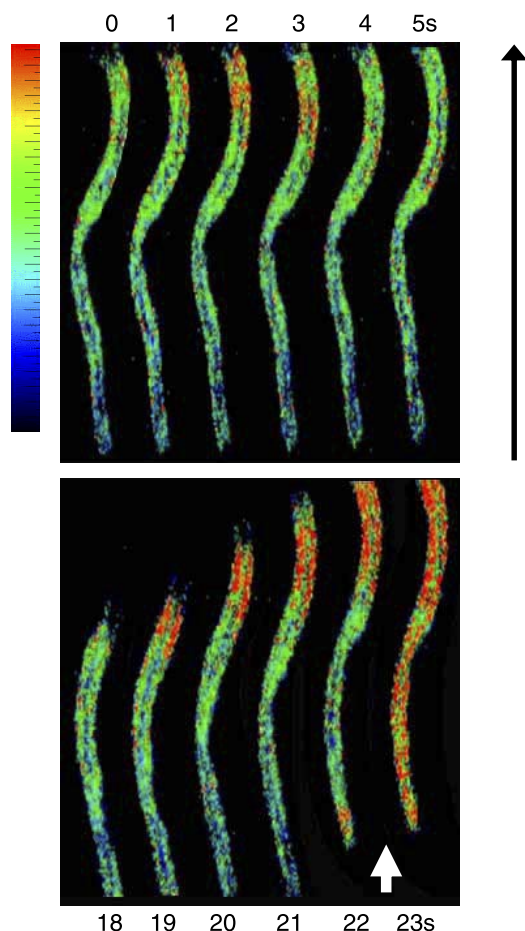
Fig. 4. Ca²⁺ wave dynamics in a *kqt-3* mutant. Pseudocolor YC6.1 535/480 nm emission ratio maps of a *kqt-3*(*tm542*) mutant at the times indicated. The oscillation in anterior intestinal cell Ca²⁺ that is shown in images on *top* (0–5 s) triggers neither the posterior cells to oscillate nor the DMP but instead delays defecation (which occurs at ~22 s, as indicated by the white arrow) by ⅓ of the "normal" cycle length. The worm is oriented with the head facing up, as shown by the black arrow.

ple targets (including the kqt channels through an inhibitory binding site). However, similar intracycle oscillations were observed as in the CaMKII mutant (Fig. 5*C*), consistent with a cell-autonomous role for CaM-CaMKII signaling in regulating Ca²⁺ flux.

Together, our data suggest that cryptic intracycle Ca²⁺ oscillations underlie the shadow cycles of *unc-43* mutants. We speculate that the defecation rhythm is maintained by a pacemaker activity that operates at several times the frequency of the cycle period and that CaMKII normally suppresses the functional response to this pacemaker, perhaps via modulating the activity of the IP₃ receptor.

The SERCA SCA-1 is required for contraction coupling during the DMP. Membrane Ca²⁺ ATPases are responsible for extruding Ca²⁺ from the cell and, in the specialized case of the sarco(endo)plasmic isoform SERCA, refilling endoplasmic reticulum (ER) stores following depletion. These proteins would be predicted to help restore intestinal cytoplasmic Ca²⁺ to baseline levels following defecation. *C. elegans* contains four membrane Ca²⁺ ATPase genes (5, 38). To test how Ca²⁺ clearance rates affect defecation, we assessed the contribution of each of the four mca (sca) genes to defecation timing using

RNAi. Because loss of *sca-1*(*mca-4*), the worm SERCA ortholog, results in embryonic and larval lethality (5, 38), we examined defecation using cell-type specific RNAi as described above to limit loss-of-function to the intestine.

To test our strain, we first treated the worms with *itr-1* RNAi. We were able to phenocopy the effects of *itr-1*(*lf*), as shown in Table 1, and intestinal Ca²⁺ oscillations were suppressed entirely relative to the control-treated animals (Fig. 6, *G* and *H*). Because *itr-1* regulates defecation via its activity in the intestine, this confirms the susceptibility of the intestine to RNAi in this rescued stain. However, the *itr-1* RNAi-treated worms were fertile (data not shown), whereas an *itr-1* deletion strain is inviable and forms dead "rod-like" larva, and N2 worms treated with *itr-1* RNAi have a pleiotropic phenotype, including larval arrest. These results further suggest that the effects of RNAi were limited to the intestine in our strain.

The *sca-1*(*RNAi*) worms grew to adulthood, and, of the four genes tested, only the *sca-1*(*RNAi*) animals had a defecation phenotype (data not shown). As might be predicted from the role of SERCA in refilling ER stores, most of the *sca-1*(*RNAi*) worms did not defecate nor did they exhibit rhythmic Ca²⁺ oscillations. Also, as demonstrated previously, the majority of animals died of an unfolded protein response (37). However, because RNAi is rarely 100% effective, a fraction of the worms continued to defecate, even as adults. For these worms, the cycle times were slightly extended compared with controls (Fig. 6, *A–C*), but the average COV was nearly the same, arguing against arrhythmia (Table 1). However, the interval between pBoc and aBoc, normally around 5 s, was greatly extended (Fig. 6, *D–F*; Table 1). Interestingly, pBoc-to-aBoc intervals were relatively consistent within a single worm from cycle to cycle, although the average pBoc-to-aBoc interval could differ dramatically between worms, which may arise from heterogeneity in the effectiveness of the RNAi treatment.

We next followed Ca²⁺ levels in the intestine and assessed when each stage of the motor program was executed relative to the changes in Ca²⁺. The amount of time that Ca²⁺ was elevated over baseline in the *sca-1*(*RNAi*) worms (Fig. 6*I*) was significantly greater than in control worms (Fig. 6*G*), consistent with a role for SERCA in Ca²⁺ clearance. In fact, although the defecation period was relatively unaltered, Ca²⁺ could remain elevated in the intestinal cells of the *sca-1*(*RNAi*) worms for up to ⅔ of the period. We also found that the pBoc contraction persisted longer than in control worms (data not shown) and that aBoc was coordinated with a reduction of Ca²⁺ levels specifically in the anterior intestinal cells, regardless of the length of the pBoc-aBoc interval (Fig. 6, *J* and *K*). The amount of time that Ca²⁺ remained elevated in the anterior intestinal cells correlated well with the pBoc-to-aBoc interval between these two contractions (Fig. 6*M*).

Because the effects of RNAi were limited to the intestine in the strain used for the experiments shown in Fig. 6, the argument can be made that the physiological role of SCA-1 in coordinating pBoc and aBoc occurs cell autonomously in the intestine. However, whether the reduction in Ca²⁺ that coincides with aBoc reflects an actual consequence of store refilling, cytoplasmic Ca²⁺ reduction, or is a result of some other facet of SERCA activity is currently unknown.
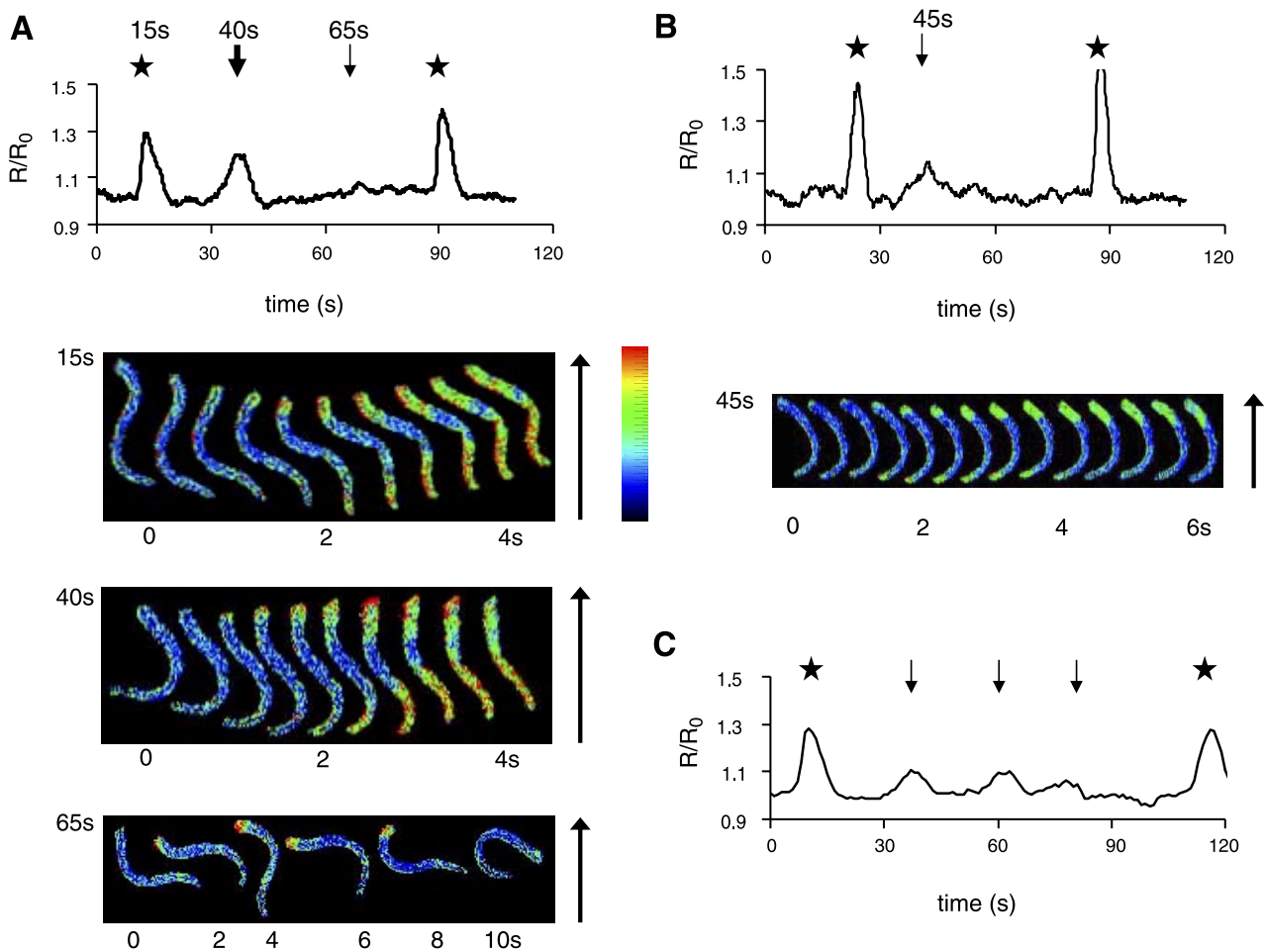
Fig. 5. Ca^{2+}/calmodulin-dependent kinase type II suppresses intracycle Ca^{2+} oscillations and reiteration of the DMP. Traces in *A* and *B* are representative intestinal Ca^{2+} oscillations from two individual *unc-43(sa200)* mutant worms. Stars denote DMP execution while arrows denote intercycle Ca^{2+} oscillations. The larger arrow in *A* indicates that a "shadow" contraction also occurred. The yellow fluorescent protein (YFP)/CFP ratio emissions maps shown below each trace depict Ca^{2+} wave dynamics at select times, as indicated. The worms are oriented with the head facing up. Trace shown in *C* is representative of intestinal Ca^{2+} oscillations following intestinal RNAi targeting *cmd-1*, which codes for the nematode calmodulin ortholog.

DISCUSSION

C. elegans are a powerful model system for studying integrated physiology, given its invariant number of cells, well-characterized behaviors, and amenability to genetic manipulation. The defecation cycle represents a robust, ultradian rhythm in the worm that is thought to be controlled by oscillatory Ca^{2+} signals in the 20 epithelial cells of the nematode intestine. By using a genetically encoded biosensor that is expressed in these cells to investigate Ca^{2+} signaling in awake, behaving worms, we uncovered novel dynamics that characterize this Ca^{2+} signal under physiological conditions. Moreover, by using this approach to characterize Ca^{2+} signaling in animals with abnormal defecation behavior, we have gained insight in the molecular mechanisms mediating Ca^{2+} wave propagation and coordinated execution of the defecation cycle.

EGL-8: insight into the molecular control of bidirectional Ca²⁺ wave propagation. We have shown that unrestrained nematodes exhibit Ca^{2+} waves that initiate simultaneously at both the anterior and posterior end of the intestine and converge around the midbody (Fig. 1). This is in contrast to previous work observing only a posterior-to-anterior Ca^{2+} wave, either coinciding with DMP execution (31) or in dis-

sected intestinal preparations (7). The discrepancy could be because of the nature of the experimental setup; in the free-range model system, worms are completely unrestrained and able to move normally on an agarose plate containing their preferred food source. We conclude that, under normal physiological conditions, two physically separate sets of intestinal cells are able to coordinately oscillate, although we are at present unable to suggest a physiological role for the reverse wave.

Our observations that the loss of PLCβ leads to ectopic Ca^{2+} waves further suggest that most, if not all, intestinal cells are capable of initiating Ca^{2+} oscillations (Fig. 2). EGL-8 has been shown to act at neuromuscular junctions in a presynaptic pathway that includes GOA-1 (G$_q$α) and UNC-13 (17) and additionally regulates several facets of male mating behavior upstream of the IP$_3$R gene *itr-1* (12). However, *egl-8* is also expressed throughout the intestine (23), with the highest expression levels observed in the posterior cells (17), and both we and others have shown that intestinal RNAi phenocopies the loss-of-function mutation, suggesting cell-intrinsic activity. Unlike its role in male mating behavior, Espelt and colleagues (7) reported that defecation arrhythmias associated with the
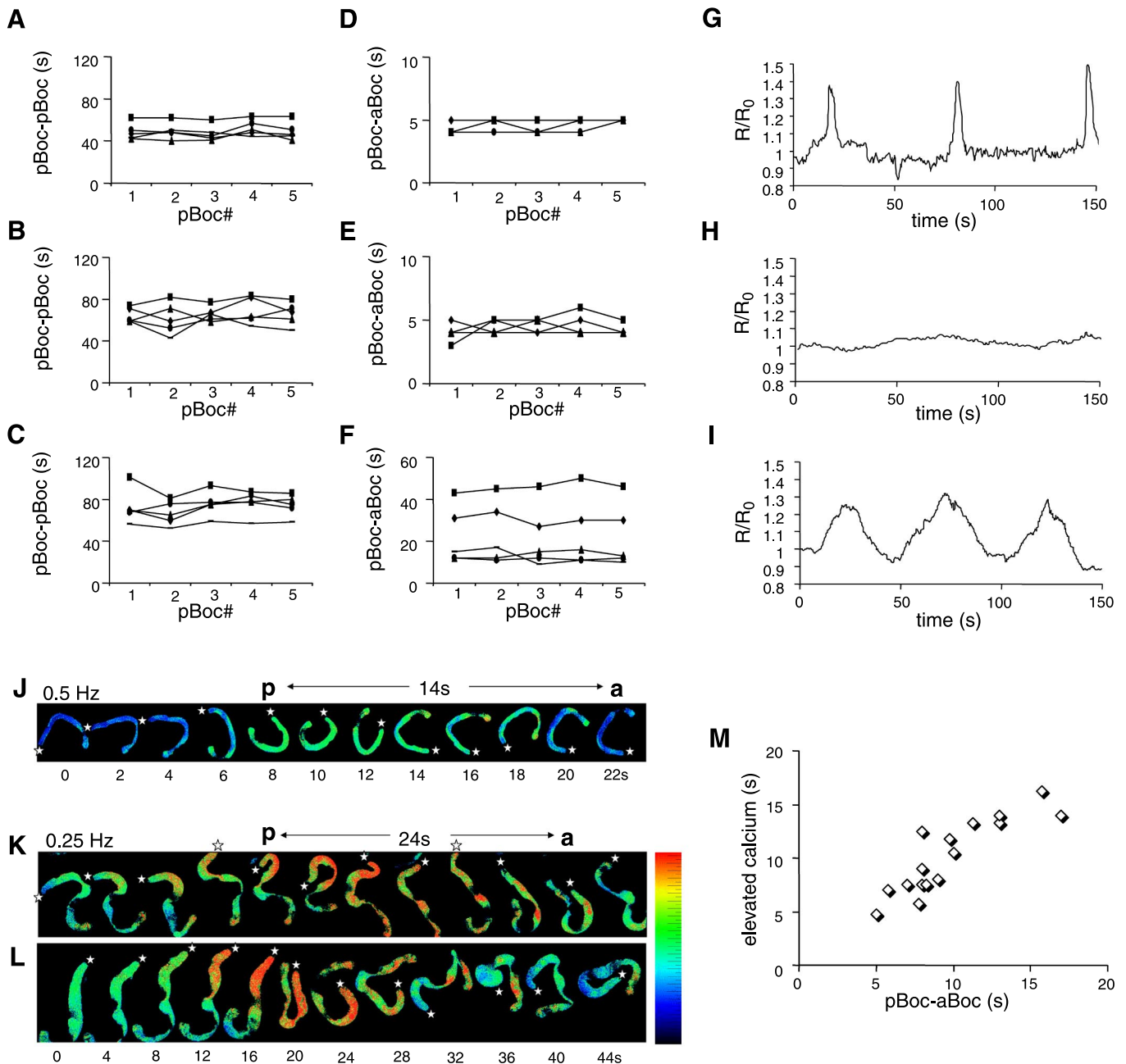
Fig. 6. Role for sarco(endo)plasmic reticulum Ca²⁺ ATPase (SERCA) and Ca²⁺ clearance in coordinating successive muscular contractions during the DMP. *A–C*: DMP cycle period; *D–F*: pBoc-to-aBoc interval for N2 worms (*A* and *D*) vs. worms where RNAi is restricted to the intestine (strain KWN15), following exposure to control (*B* and *E*) or *sca-1* RNAi (*C* and *F*). Note that the scale in *F* differs from that in *D* and *E*. Although the cycle period is similar for *sca-1*(*RNAi*) and control worms, the timing of aBoc relative to pBoc appears to be altered. *G–I*: average Ca²⁺ oscillations following control, *itr-1*, or *sca-1* RNAi, respectively. *J–L*: pseudocolor YC6.1 YFP/CFP emission ratio maps for intestine-restricted RNAi worms treated with *sca-1* RNAi. Stars were placed at the posterior end of the intestine in each panel for orientation. The series in *K* and *L* show two successive cycles from the same worm at 0.25 Hz, whereas the series in *J* is shown at 0.5 Hz. M, period that Ca²⁺ remained elevated over baseline (defined at a relative value of 1.1 times resting levels) plotted against the pBoc-to-aBoc interval for 15 separate worms treated with *sca-1* RNAi.

loss-of-function mutation could not be suppressed by a gain-of-function mutation in *itr-1*, and the failure of exogenous DAG to suppress the arrhythmia argued against a function analogous to its role in neurotransmission, as well.

So how does EGL-8 regulate defecation? In many systems, PLCβ acts downstream of G protein-coupled receptors. Also, in fact, the Rho/Rac family GEF VAV-1 has been shown to regulate multiple rhythmic behaviors in worms, including def-

ecation. Moreover, the Rho/Rac small GTPases *ced-10*, *mig-2*, and *rho-1* also have redundant functions in structuring the defecation rhythm (25). However, the loss of VAV-1 can be suppressed by an *itr-1* gain-of-function mutation and VAV-1 has been shown to act upstream of PIP5K, which generates PIP₂, the substrate for IP₃ production (25). These results suggest that VAV-1 may function in the same pathway as PLCγ to generate substrate for the IP₃R, rather than the PLCβ

pathway. In support of this idea, we find that intestinal RNAi of *vav-1* results in arrhythmia (Table 1) but that Ca^{2+} oscillations in the intestine nonetheless initiate in both anterior and posterior cells, as normal; the same is true for *ced-10*, *mig-15*, and *rho-1* (data not shown). Instead, EGL-8 may act primarily to deplete PIP_2 rather than to generate IP_3. PIP_2 (along with PIP_3) has been shown to target many proteins to the plasma membrane, including Ras, Rab, Arf, and Rho proteins (15).

It has also been suggested that PLC acts as a positive feedback mechanism during stimulation-induced Ca^{2+} oscillations because its activity is increased by cytosolic Ca^{2+} and that this feedback would result in regenerative IP_3 oscillations that fuel spikes in Ca^{2+} (22). The *egl-8*(*lf*) phenotype is consistent with such a role for this gene. If *egl-8* activity served to set a threshold for regenerative spiking, spatial heterogeneity in the activity of this gene would be expected to result in preferred sites of wave initiation. Indeed, *egl-8* is most highly expressed in the posterior intestinal cells, which have been consistently identified as a primary site of wave initiation in numerous studies. Furthermore, a reduction of *egl-8* activity would be expected to result in spatially unpredictable and arrhythmic Ca^{2+} spikes, as is indeed observed with *egl-8*(*lf*). However, it remains unclear as to why *egl-8* would preferentially play this role instead of *plc-3*.

A very recent report describes the role of the worm intestinal pannexin gap-junction protein INX-16 on Ca^{2+} wave oscillations (27). Intriguingly, the arrhythmia and random or reverse wave propagation described in this report mirrors closely the ectopic Ca^{2+} oscillations that we observe in the *egl-8*(*lf*) mutant. Although this is an important independent confirmation of our hypothesis that all intestinal cells are capable of initiating a Ca^{2+} wave, it also raises the question of whether one role of EGL-8 may be to regulate INX-16 or gap-junction behavior. In future work, the Ca^{2+} oscillation phenotype that we have identified in *egl-8* mutants will undoubtedly help to differentiate between mechanistically distinct physiological regulators of the defecation rhythm and elucidate the signaling pathways in which they function.

Ca²⁺ oscillation dynamics and rhythmicity in the defecation cycle: the role of KQT channels. In addition to IP_3-mediated release of Ca^{2+} from internal stores, Ca^{2+} influx from outside the cell is also required for generation of Ca^{2+} oscillations in the intestine, although the molecular pathway that mediates Ca^{2+} entry remains unknown (19, 37). Noting the defecation and Ca^{2+} oscillation phenotypes observed in the kqt mutants, we postulate that KQT channels regulate Ca^{2+} entry through the generation of a strong electrical driving force. We propose the following model: Ca^{2+} entry and/or IP_3 generation by PLC evokes Ca^{2+}-induced Ca^{2+} release (CICR) and a spike in intracellular Ca^{2+} levels. Following this increase, Ca^{2+} inhibits KQT channel activity through CaM, which is bound to the IQ motif present in these channels. Feedback inhibition of KQT channel activity then depolarizes the resting potential and suppresses Ca^{2+} influx. Reduced Ca^{2+} entry and sequestration/buffering of intracellular Ca^{2+} relieves Ca^{2+}-dependent KQT channel inhibition and restores the driving force for plasma membrane Ca^{2+} entry for the next cycle of IP_3-evoked CICR from internal stores.

Three predictions follow from our working model. If KQT channels regulate plasma membrane Ca^{2+} influx required for activation and termination of CICR, then disrupting KQT

channel function should *1*) augment the duration of Ca^{2+} oscillations and *2*) diminish the onset and *3*) diminish the amplitude of Ca^{2+} spikes. As shown in Fig. 3, Ca^{2+} oscillation duration in kqt mutants is two to three times longer than that of wild-type animals (also see supplemental Fig. S4). Consistent with the role of CaM in our model, the oscillations following *cmd-1* RNAi appear to be extended compared with the wild type, as well (Fig. 5). We also observe a slow onset of the Ca^{2+} increase in both of the kqt mutants, potentially reflecting the uncoupling of plasma membrane Ca^{2+} influx and IP_3 generation and dysregulation of CICR. Finally, our model is further supported by the observation of small-amplitude Ca^{2+} signals, which often failed to evoke body wall muscle contractions. We postulate that these nonproductive Ca^{2+} transients represent Ca^{2+} release from internal stores that fail to develop into full-amplitude Ca^{2+} oscillations. This could be attributed to an uncoupling of plasma membrane Ca^{2+} influx and Ca^{2+} liberation from the ER. We note that these nonproductive Ca^{2+} oscillations in particular are often more persistent than oscillations that are linked to the DMP (for example, see Fig. 5), suggesting that the speed of Ca^{2+} increase is directly related to the time it remains elevated.

Intestinal Ca²⁺ waves coordinate execution of the DMP. Our observations suggest that the posterior-to-anterior wave is a necessary precursor to execution of the complete DMP and that wave directionality is important for functional coupling of the muscular contractions (Fig. 2). In none of the strains examined in our study did we observe the initiation of the DMP in the absence of the posterior-to-anterior wave [although a weak pBoc alone was triggered in the *egl-8*(*lf*) mutant during reverse waves that traveled through the posterior intestine, but in the wrong direction]. Moreover, the extent of posterior-to-anterior wave propagation was positively correlated with successful execution of the full DMP. Indeed, examination of the shadow cycle *unc-43*(*sa200*) mutants suggested the existence of dependencies between the anterior and posterior oscillations and the execution of the DMP. Strong Ca^{2+} oscillations in the anterior cells correlated with Ca^{2+} oscillations in the posterior cells and the execution of pBoc, whereas weak oscillations in the anterior cells did not. Furthermore, pBoc was followed by aBoc only when Ca^{2+} oscillations in the posterior cells propagated in the form of a wave. Similar observations were made regarding the "abortive" anterior oscillations of kqt mutants. These results are consistent with the observation that injection of heparin, an IP_3R inhibitor, in int5 prevented Ca^{2+} wave propagation as well as the latter steps in the DMP (31). However, because anterior-to-posterior waves were not observed in that study, it seems either that they are not strictly required for posterior-to-anterior wave propagation or execution of the DMP or that the model system in use did not facilitate their detection.

Further insight into the role of Ca^{2+} in coordinating the DMP in free-range worms was gained by investigating the effects of RNAi on the four *C. elegans* membrane Ca^{2+} ATPases. Of these four genes (*mca-1, mca-2, mca-3,* and *sca-1*), only *sca-1*, the worm SERCA ortholog, appeared to control Ca^{2+} dynamics in the intestine and the defecation phenotype. Because *sca-1* RNAi resulted in a high degree of lethality, as reported previously (5, 38), we used intestine-restricted RNAi to test its function specifically during Ca^{2+} oscillations associated with defecation. As expected, knock

down of the SERCA ortholog increased the duration of cytoplasmic Ca^{2+} oscillations. To our surprise, however, the defecation period was only slightly affected by *sca-1* RNAi, regardless of how long Ca^{2+} remained elevated (Fig. 6). Instead, we observed that the timing between pBoc and aBoc was affected. We had noted previously that aBoc appeared to coincide with the return of Ca^{2+} in the anterior intestinal cells to baseline levels (Fig. 1). In the *sca-1(RNAi)* worms, the prolonged elevation in Ca^{2+} resulted in a lengthened interval between pBoc and aBoc (Fig. 6). Furthermore, aBoc always occurred as Ca^{2+} in the anterior cells returned to normal levels, regardless of the amount of time that it was elevated (Fig. 6). We made similar observations in *kqt* mutant worms, which also have slightly but significantly increased pBoc-to-aBoc intervals (Table 1) that are coincident with prolonged Ca^{2+} oscillations (Fig. 3).

We suggest a model where the temporal coupling between successive muscular contractions is determined, at least in part, by how quickly Ca^{2+} diminishes following oscillations. Because reduction-of-function following *sca-1* RNAi was restricted to the intestine, it is unlikely that the alteration in DMP timing is the result of Ca^{2+} dynamics being misregulated in other tissues. How this relates to the signals that pass between the intestine and the neurons to signal the anterior body wall and enteric muscles to contract is at this time unknown but likely rules out a conventional Ca^{2+}-induced vesicle fusion event.

"Arrhythmic" phenotypes and the case for an underlying pacemaker. Investigation of the relationships between altered Ca^{2+} wave dynamics and arrhythmic defecation cycle phenotypes has led us to hypothesize the existence of an underlying pacemaker activity. This hypothesis has been motivated in part by our observation of unexpected regularities in the defecation cycle of arrhythmic mutants. We have found that arrhythmic events occur with a consistent relationship vis-à-vis the normal defecation rhythm in several mutant backgrounds. In both *unc-43(sa200)* mutants and animals treated with *cmd-1* RNAi, we observed shadow cycles that occurred at ~⅓ the duration of the normal defecation cycle (Fig. 4). In *kqt* mutant animals, we observed that abortive anterior Ca^{2+} oscillations were accompanied by an offset of the DMP equivalent to ~⅓ of the defecation period (Fig. 3). Whether the cycle is extended or abbreviated, arrhythmic events fell in reproducible intervals at a fraction the length of the typical defecation cycle with unexpected frequency. Together, these observations suggest that the defecation phenotypes of these mutants results from uncoupling of the pacemaker from the DMP, rather than disruption of pacemaker activity itself, implying that Ca^{2+} oscillations may be in fact a response to an underlying, higher-frequency pacemaker activity.

Model of a molecular pacemaker. These observations have also led us to question how Ca^{2+} regulates the defecation period. It is presumed that there must be an underlying biological activity that unfolds with a time course appropriate to yield the periodicity of the defecation cycle. It is notable that, although intestinal Ca^{2+} oscillations have been observed to correlate with the defecation cycle, these oscillations are discrete in nature and thus represent at best an incomplete observation of the biological process serving as the pacemaker. Indeed, to date, no continuously varying biological signal has

been identified as a candidate pacemaker activity for the defecation cycle.

It is possible that fluctuations in Ca^{2+} levels below the level of detection of our YC biosensor constitute such a signal. Espelt et al. (7) recently reported that, under specific voltage-clamp conditions, isolated intestinal cells exhibit a continuously oscillating TRP-like current, offering a possible mechanism through which subrosa Ca^{2+} oscillations may contribute to the pacemaker activity. It is also of note that the *itr-1(sa73)* mutation that causes an extended defecation period occurs in a putative Ca^{2+}-binding domain and can be compensated for by increasing extracellular Ca^{2+} (7), consistent with the idea that undetected Ca^{2+} flux contributes to timing the defecation cycle. However, given that high levels of cytosolic Ca^{2+} are thought to repress IP$_3$R activity, our *sca-1* results suggest that this repression at least is not an essential component of the pacemaker.

In light of our analysis of arrhythmic mutants, we favor a model where a distinct underlying pacemaker oscillation triggers Ca^{2+} influx when a threshold value is reached, as via temporal summation. Given that the influx of Ca^{2+} requires activation of the IP$_3$R, it is possible that oscillations in IP$_3$ itself act as the pacemaker. Of course, because low levels of Ca^{2+} can enhance the activity of the IP$_3$R, it is also possible small rhythmic increases in Ca^{2+} occur such that both IP$_3$ and Ca^{2+} oscillations contribute to the pacemaking activity. As noted above, PLC could act as part of a positive feedback mechanism during Ca^{2+} oscillations (24), and our observations of ectopic wave initiation in *egl-8* mutants are consistent with this idea. However, our *sca-1* data hint that Ca^{2+} stimulation of PLC activity may not be primarily responsible for determining the temporal oscillatory pattern in the defecation system. Critical assessment of the validity of this model will require the use of transgenic strains expressing IP$_3$-sensitive biosensors such as LIBRA or IRIS (20, 30).

REFERENCES

1. **Berridge MJ, Bootman MD, Roderick HL.** Calcium signaling: dynamics, homeostasis and remodelling. *Nat Rev Mol Cell Biol* 4: 517–529, 2003.
2. **Branicky R, Hekimi S.** What keeps *C. elegans* regular: the genetics of defecation. *Trends Genet* 22: 571–579, 2006.
3. **Branicky R, Shibata Y, Feng J, Hekimi S.** Phenotypic and suppressor analysis of defecation in clk-1 mutants reveals that reaction to changes in temperature is an active process in Caenorhabditis elegans. *Genetics* 159: 997–1006, 2001.
3a. **Brenner S.** The genetics of *Caenorhabditis elegans. Genetics* 77: 71–94, 1974.
4. **Charlie NK, Schade MA, Thomure AM, Miller KG.** Presynaptic UNC-31 (CAPS) is required to activate the G alpha(s) pathway of the Caenorhabditis elegans synaptic signaling network. *Genetics* 172: 943–961, 2006.

5. **Cho JH, Bandyopadhyay J, Lee J, Park CS, Ahnn J.** Two isoforms of sarco/endoplasmic reticulum calcium ATPase (SERCA) are essential in Caenorhabditis elegans. *Gene* 261: 211–219, 2000.

6. **Dal Santo P, Logan M, Chisholm A, Jorgensen E.** The inositol triphosphate receptor regulates a 50-second behavioral rhythm in *C. elegans. Cell* 98: 757–767, 1999.

7. **Espelt M, Estevez A, Yin X, Strange K.** Oscillatory Ca2+ signaling in the isolated *Caenorhabditis elegans* intestine: role of the inositol-1,4,5-trisphosphate receptor and phospholipases C β and γ. *J Gen Physiol* 126: 379–392, 2005.

8. **Faumont S, Lockery SR.** The awake behaving worm: simultaneous imaging of neuronal activity and behavior in intact animals at millimeter scale. *J Neurophysiol* 95: 1976–1981, 2006.

9. **Faumont S, Miller AC, Lockery SR.** Chemosensory behavior of semi-restrained *Caenorhabditis elegans. J Neurobiol* 65: 171–178, 2005.

10. **Ferrari MB, Spitzer NC.** Calcium signaling in the developing *Xenopus* myotome. *Dev Biol* 213: 269–282, 1999.

11. **Gomez TM, Snow DM, Letourneau PC.** Characterization of spontaneous calcium transients in nerve growth cones and their effect on growth cone migration. *Neuron* 14: 1233–1246, 1995.

12. **Gower NJ, Walker DS, Baylis HA.** Inositol 1,4,5-trisphosphate signaling regulates mating behavior in *Caenorhabditis elegans* males. *Mol Biol Cell* 16: 3978–3986, 2005.

13. **Granato M, Schnabel H, Schnabel R.** pha-1, a selectable marker for gene transfer in *C. elegans. Nucleic Acids Res* 22: 1762–1773, 1994.

14. **Hagen FK, Nehrke K.** cDNA cloning and expression of a family of UDP-N-acetyl-D-galactosamine:polypeptide N-acetylgalactosaminyltransferase sequence homologs from Caenorhabditis elegans. *J Biol Chem* 273: 8268–8277, 1998.

15. **Heo WD, Inoue T, Park WS, Kim ML, Park BO, Wandless TJ, Meyer T.** PI(3,4,5)P3 and PI(4,5)P2 lipids target proteins with polybasic clusters to the plasma membrane. *Science* 314: 1458–1461, 2006.

16. **Jee C, Lee J, Lee J, Lee W, Park B, Yu J, Park E, Kim E, Ahnn J.** SHN-1, a Shank homologue in *C. elegans*, affects defecation rhythm via the inositol-1,4,5-trisphosphate receptor. *FEBS Lett* 561: 29–36, 2004.

17. **Lackner M, Nurrish S, Kaplan J.** Facilitation of synaptic transmission by EGL-30 G(q)alpha and EGL-8 PLC beta: DAG binding to UNC-13 is required to stimulate acetylcholine release. *Neuron* 24: 335–346, 1999.

18. **Liu D, Thomas J.** Regulation of a periodic motor program in C. *elegans. J Neurosci* 14: 1953–1962, 1994.

19. **Lorin-Nebel C, Xing J, Yan X, Strange K.** CRAC channel activity in *C. elegans* is mediated by Orai1 and STIM1 homologues and is essential for ovulation and fertility. *J Physiol* 580: 67–85, 2007.

20. **Matsu-ura T, Michikawa T, Inoue T, Miyawaki A, Yoshida M, Mikoshiba K.** Cytosolic inositol 1,4,5-trisphosphate dynamics during intracellular calcium oscillations in living cells. *J Cell Biol* 173: 755–765, 2006.

21. **Mello CC, Kramer JM, Stinchcomb D, Ambros V.** Efficient gene transfer in *C. elegans*: extrachromosomal maintenance and integration of transforming sequences. *EMBO J* 10: 3959–3970, 1991.

22. **Meyer T, Stryer L.** Molecular model for receptor-stimulated calcium spiking. *Proc Natl Acad Sci USA* 85: 5051–5055, 1988.

23. **Miller K, Emerson M, Rand J.** G(o)alpha and diacylglycerol kinase negatively regulate the G(q)alpha pathway in *C. elegans. Neuron* 24: 323–333, 1999.

24. **Nehrke K, Melvin JE.** The NHX family of Na+-H+ exchangers in Caenorhabditis elegans. *J Biol Chem* 277: 29036–29044, 2002.

25. **Norman K, Fazzio R, Mellem J, Espelt M, Strange K, Beckerle M, Maricq A.** The Rho/Rac-family guanine nucleotide exchange factor VAV-1 regulates rhythmic behaviors in C. *elegans. Cell* 123: 119–132, 2005.

26. **Ozil JP, Swann K.** Stimulation of repetitive calcium transients in mouse eggs. *J Physiol* 483: 331–346, 1995.

27. **Peters MA, Teramoto T, White JQ, Iwasaki K, Jorgensen EM.** A gap-junction-mediated calcium wave coordinates a rhythmic behavior in *C. elegans. Curr Biol* doi:10.1016/j. cub.2007.08.031, 2007.

28. **Reiner D, Newton E, Tian H, Thomas J.** Diverse behavioural defects caused by mutations in *Caenorhabditis elegans* unc-43 CaM Kinase II. *Nature* 402: 199–203, 1999.

29. **Siklos S, Jasper J, Wicks S, Rankin C.** Interactions between an endogenous oscillator and response to tap in C. *elegans. Psychobiology* 28: 571–580, 2000.

30. **Tanimura A, Nezu A, Morita T, Turner RJ, Tojyo Y.** Fluorescent biosensor for quantitative real-time measurements of inositol 1,4,5-trisphosphate in single living cells. *J Biol Chem* 279: 38095–38098, 2004.

31. **Teramoto T, Iwasaki K.** Intestinal calcium waves coordinate a behavioral motor program in *C. elegans. Cell Cal* 40: 319–327, 2006.

32. **Thomas J.** Genetic analysis of defecation in *Caenorhabditis elegans. Genetics* 124: 855–872, 1990.

33. **Truong K, Sawano A, Mizuno H, Hama H, Tong KI, Mal TK, Miyawaki A, Ikura M.** FRET-based in vivo Ca2+ imaging by a new calmodulin-GFP fusion molecule. *Nat Struct Biol* 8: 1069–1073, 2001.

34. **Uhlâen P, Laestadius A, Jahnukainen T, Sèoderblom T, Bèackhed F, Celsi G, Brismar H, Normark S, Aperia A, Richter-Dahlfors A.** Alpha-haemolysin of uropathogenic E coli induces Ca2+ oscillations in renal epithelial cells. *Nature* 405: 694–697, 2000.

35. **Walker D, Ly S, Lockwood K, Baylis H.** A direct interaction between IP3 receptors and myosin II regulates IP3 signaling in *C. elegans. Curr Biol* 12: 951–956, 2002.

36. **Wei AD, Butler A, Salkoff LA, Department of Neurobiology.** KCNQ-like potassium channels in*Caenorhabditis elegans* conserved properties and modulation. *J Biol Chem* 280: 21337–21345, 2005.

37. **Yan X, Xing J, Lorin-Nebel C, Estevez AY, Nehrke K, Lamitina T, Strange K.** Function of a STIM1 homologue in *C. elegans*: evidence that store-operated Ca2+ entry is not essential for oscillatory Ca2+ signaling and ER Ca2+ homeostasis. *J Gen Physiol* 128: 443–459, 2006.

38. **Zwaal RR, Van Baelen K, Groenen JT, van Geel A, Rottiers V, Kaletta T, Dode L, Raeymaekers L, Wuytack F, Bogaert T.** The sarco-endoplasmic reticulum Ca2+ ATPase is required for development and muscle function in *Caenorhabditis elegans. J Biol Chem* 276: 43557–43563, 2001.